



# Research on Improving the Spatial Arrangement of Dampers Based on Multi-Objective Optimization

Chuang Peng, Bei Xiong\*, Xinran Li

Chongqing College of Architecture and Technology, Chongqing, 401331, China

\*Corresponding author: XB2016020108@cqrec.edu.cn

**Abstract.** The research aims to optimize viscous damper-based seismic reinforcement for single-span reinforced concrete frame structures. In this case, the fast non-dominated sorting genetic algorithm II (NSGA-II) based on multi-objective optimization is adopted to improve the crossover operator and the mutation operator in the algorithm, so as to ensure that the numbers of specific genes in the chromosomes remain the same across generations. Also, the research analyzes the variation curves of the objective functions with the increasing number of dampers when a structure is under three different seismic waves, thereby proposing a theory for selecting more economical reinforcement schemes on the premise that the structure's safety is guaranteed. At last, it explores the damping effects of different Pareto optimal solutions suggested by the improved NSGA-II under three seismic waves to provide a reference for the spatial arrangement of dampers in single-span reinforced concrete frame structures.

**Keywords:** Damping; Single-Span Reinforced Concrete Frame; Damper; NSGA-II; Reinforcement.

## 1 Introduction

Currently, the installation of additional dampers on existing structures has become the mainstream solution for seismic reinforcement. The Beijing Railway Station and the Beijing Hotel, which were originally designed without the consideration of earthquake fortification, adopted viscous dampers for subsequent reinforcement<sup>[1]</sup>. The R&D building of the Changqing Petroleum Exploration Bureau in Xi'an, Shaanxi, employed 20 dampers to reduce its structural response under seismic and wind loads<sup>[2]</sup>. The Hefei TV Tower used viscous dampers to mitigate the displacement and acceleration response of the tower under strong earthquakes<sup>[3]</sup>. These cases suggest that dampers applied as structural reinforcement units can effectively reduce the dynamic response under wind loads and earthquakes.

Early studies on the damper-based energy dissipation solution argued that for high-rise buildings, viscous dampers should be deployed evenly on each storey. However, as the numbers of both storeys and dampers increase, the spatial arrangement of dampers becomes one of the primary challenges in improving the performance of energy

dissipation. In recent years, many researchers have tried to employ straightforward continuous searching, topology optimization, and gradient-based methods to optimize the damper arrangement.

Zhang<sup>[4]</sup> and CHEN<sup>[5]</sup> adopted the genetic algorithm based on Darwin's theory of evolution to optimize the damper arrangement for vertical planes. In general, most existing studies aimed to optimize the arrangement of dampers on a plane, whereas few emphasized the spatial optimization of dampers for overall structures.

In China, a majority of elementary and secondary schools are subject to the single-span reinforced concrete frame for its structural function, which boasts better seismic performance and more usable space. However, in the Wenchuan earthquake on May 12, 2008, the teaching buildings subject to this frame were severely damaged, endowing the research efforts on reducing the seismic response of existing single-span reinforced concrete frame structures with critical engineering significance.

Above, in the case of single-span reinforced concrete frame structures, this research aims to explore how to deploy dampers in a space frame structure to improve its seismic performance. The non-dominated sorting genetic algorithm II (NSGA-II) <sup>[6]</sup> and ANSYS, a large-scale finite element software, are introduced to program an optimizer for the damper arrangement in a space frame structure. The optimizer takes the maximum acceleration and the maximum inter-storey drift of single-span reinforced concrete frame structures as the dual-control indicators for multi-objective optimization. The calculations suggest that reinforcement solutions generated by the improved NSGA-II can realize conspicuous damping performance for single-span reinforced concrete frame structures under different seismic waves.

## 2 Principle of NSGA-II

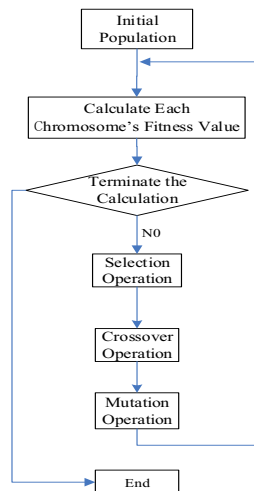


**Fig. 1.** Workflow of the Genetic Algorithm

The NSGA-II is a new genetic algorithm developed based on Darwin's theory of evolution and Mendelism. Mainly applied for the optimization of complex systems, the genetic algorithm was first suggested by Professor Holland (American), which is a population-based, efficient, and parallel method for global searching in essence. At present, it has been applied successfully in the optimization of frame structure [7], fluid viscous dampers could be employed to reinforce an existing building [8], and other fields, indicating the algorithm's effectiveness and applicability in engineering optimization.

In the genetic algorithm, the vectors to be optimized are known as chromosomes or individuals. At first, a population consisting of  $M$  chromosomes is generated through random operation. Then, based on the selected objective functions, the fitness value (also called the objective function value) of each chromosome can be calculated. Next, by virtue of selection operation, crossover operation, and mutation operation, new chromosomes with higher fitness values can be generated continuously, allowing the population to move towards the optimal solution. The workflow of a genetic algorithm is illustrated in Fig. 1 [9].

### 3 Improvement and Optimization of NSGA-II

#### 3.1 Improvement of NSGA-II

In 2002, Professor Kalyanmoy Deb proposed the NSGA-II [6] on the basis of the first-generation NSGA, which significantly improved the conventional genetic algorithm's performance by integrating the fast non-dominated sorting, the crowding distance, and the elitist preservation strategy.

**Fast Non-Dominated Sorting Algorithm.** The basic logic of the non-dominated sorting algorithm is to allocate the non-dominated solutions in the solution space to a specific layer to separate the space into different layers, so as to obtain the Pareto optimal solution. It is a process of solving the multiple-objective optimization problem. The primary steps are shown below:

Step 1: Based on the Pareto dominance principle, each individual ( $p$ ) in the population involves two parameters –  $S_p$  and  $n_p$ .  $S_p$  is the set of individuals that are dominated by  $p$ , and  $n_p$  is the number of individuals that dominate  $p$ ;

Step 2: Search for all individuals subject to " $n_p = 0$ " in the population, store them in the first layer ( $F_1$ ), and assign them with the corresponding non-dominated rank ( $I_{\text{rank}}$ );

Step 3: Assuming Set  $Q = \text{null}$ , traverse each individual ( $P_i$ ) that is dominated by each individual ( $P_j$ ) in the  $i^{\text{th}}$  layer ( $F_i$ ). For  $P_i$ , execute operation " $n_p = n_{p-1}$ ". If  $n_p = 0$ , store  $P_i$  in Set  $Q$ ;

Step 4: Terminate the algorithm once all individuals in the population are marked and allocated to  $F_i$ ;

Step 5: Assuming  $i = i + 1$ , note  $F_i = Q$ , and go to Step 3.

**Crowding Distance.** The NSGA-II can allocate the non-inferior solutions in the solution space to a specific layer to allow for convenient selection operation on different

layers. However, a layer may involve many individuals, which necessitates a uniform fitness value for all individuals in the same layer to perform selection operations. In this context, the NSGA-II is the first algorithm to propose the crowding distance concept, which is defined as the local distance of each point to its two neighboring points in the same layer in the objective space. For instance, in the dual-objective optimization function (Fig. 2), the crowding distance of the  $i^{\text{th}}$  point is equal to the sum of its neighboring points in the same layer –  $i-1$  and  $i+1$  – on Objective Functions  $f_1$  and  $f_2$ . In other words, it is equal to the perimeter of the rectangle composed of Points  $i-1$  and  $i+1$ . Using a virtual fitness value, a selection operation can be executed for the individuals from the same layer, allowing for evener individual selection in the objective space to ensure higher robustness of the final calculation results.

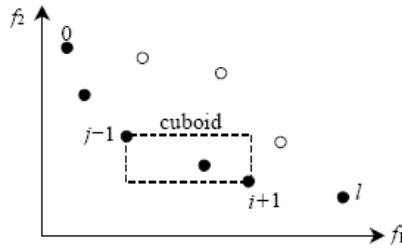


Fig. 2. Local Crowding Distance of the Dual-Objective Optimization Function

**Elitist Preservation Strategy** [10]. It has been shown that the genetic algorithm integrated with the elitist preservation strategy can converge to the Pareto optimal solution in a shorter period. Thus, the NSGA-II is capable of preserving the parents with fine genes directly in the filial generation. This procedure is considered as the elitist preservation strategy, and the steps include:

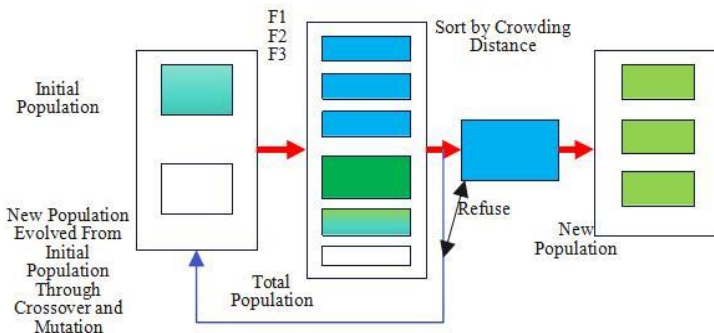


Fig. 3. Framework of the NSGA-II’s Elitist Preservation Strategy

Step 1: Unit the  $N$ -sized parental generation ( $P_t$ ) and the  $N$ -sized filial generation ( $Q_t$ ) into a  $2N$ -sized population ( $R_t$ );

Step 2: Adopt the fast non-dominated sorting algorithm to acquire the ranks of non-inferior solutions and the crowding distance of the new population ( $R_t$ );

Step 3: Select individuals according to the ranking of the non-inferior solutions, with the lowest layers entering into the new parent population ( $P_{t+1}$ ) until the size of the population reaches  $N$ ;

Step 4: In cases where all individuals from a particular rank cannot enter into  $P_{t+1}$ , the individuals can be sorted alternatively according to their crowding distances, with priority for those with greater crowding distances.

The calculation process is illustrated in Fig. 3.

**Improvement of the Crossover and Mutation Operators.** For binary coding, the genetic locus is  $\{0,1\}$ , with 0 indicating no damper should be deployed at this position and 1 indicating one damper should be deployed at this position.

The crossover and mutation operators are the most important genetic operators in the genetic algorithm. According to the building block hypothesis, while the crossover operator produces offspring by recombining the parents' characteristics, the mutation operator produces offspring with new genetic characteristics by mutating the parents' genes. Both are genetic operations. The locus of a binary-coded chromosomal gene is  $\{0,1\}$ . An improvement of the crossover and mutation operators is required to ensure that a particular chromosome has given numbers of  $\{0\}$  and  $\{1\}$  genes, that the numbers of  $\{0\}$  and  $\{1\}$  genes remain unchanged, and that the offspring produced based on the parents via the crossover and mutation operators possess the parents' fine genes. The improvement steps for the crossover operator are stipulated:

Step 1: Select two individuals randomly from the parent population for crossover operation;

Step 2: Identify the numbers and positions of  $\{0\}$  and  $\{1\}$  genes in the two parental generations;

Step 3: Generate random numbers within the range of the numbers and positions of  $\{0\}$  and  $\{1\}$  genes in the parental generations;

Step 4: Perform crossover operation between the positions of  $\{0\}$  genes in Parental Generation 1 and the positions of  $\{1\}$  genes in Parental Generation 2. Perform crossover operation between the positions of the  $\{1\}$  genes in Parental Generation 1 and the positions of the  $\{0\}$  genes in Parental Generation 2.

The crossover operator is improved based on the binary single-point crossover, which ensures that the numbers of  $\{0\}$  and  $\{1\}$  genes in the filial generation are always equal to that in the parental generation.

For the regular crossover operator, the two parent individuals chosen for crossover operation can be:

Parent  $X_1$ : 0 1 0 1 1 | 0 1 0 0 1

Parent  $X_2$ : 1 0 0 1 0 | 1 0 1 0 1

If the vertical bar in the gene string is considered the crossover position, the new individuals produced via crossover operation can be:

Offspring  $X_1'$ : 0 1 0 1 1 | 1 0 1 0 1

Offspring  $X_2'$ : 1 0 0 1 0 | 0 1 0 0 1

For the improved crossover operator, the parent individuals are the same as the regular ones:

Parent X<sub>1</sub>: 0 1 0 1 1 0 1 0 0 1  
                   ↑↑↑          ↑↑          ↑↑  
                   ↓↓↓          ↓↓          ↓↓  
 Parent X<sub>2</sub>: 1 0 0 1 0 1 0 1 0 1  
 The new individuals produced can be:  
 Offspring X<sub>1</sub>' : 1 0 0 1 0 0 1 1 0 1  
 Offspring X<sub>2</sub>' : 0 1 0 1 1 1 0 0 0 1

Similarly, to ensure that the numbers of the {0} and {1} genes of the mutated offspring remain unchanged, the mutation operator can be improved following the steps below:

Step 1: Traverse all the genes on the parental chromosome and employ one or some of them as the mutation sites with a low probability;

Step 2: Locate the positions of {1} and {0} genes in the chromosome;

Step 3: Mutate one {1} gene in the chromosome to a {0} gene, and then concurrently, mutate {0} gene to a {1} gene.

For the regular mutation operator:

Parent A:           0 1 0 1 1 0 1 0 0 1  
                       ↓                          ↓                          ↓  
                       ↓                          ↓                          ↓  
 Offspring B:       1 1 0 1 1 1 1 0 0 0

For the improved mutation operator:

Parent A:           0 1 0 1 1 0 1 0 0 1  
                       ↓          ↓          ↓          ↓  
                       ↓          ↓          ↓          ↓  
 Parent A:           0 0 0 0 1 1 1 0 1 1

### 3.2 Optimized Spatial Arrangement of Dampers

Viscous dampers are often arranged in series with diagonal bracings in the interlayers of a structure. In general, the force of a linear viscous damper depends on the magnitude of its instantaneous relative velocity<sup>[11]</sup>:

$$F(t) = -c_{eq} \dot{u}(t) \tag{1}$$

In the case of seismic motion, the differential equation of motion of a structure equipped with viscous dampers can be expressed as:

$$[M] \{\ddot{u}(t)\} + ([C] + [C_z]) \{\dot{u}(t)\} + [K] \{u(t)\} = -[M] \{I\} \ddot{x}_g(t) \tag{2}$$

where [M] is the major structure's mass, [C] is the major structure's damping, [K] is the major structure's stiffness matrix,  $\{\ddot{u}(t)\}$  is the major structure's accelerated velocity,  $\{\dot{u}(t)\}$  is the major structure's velocity,  $\{u(t)\}$  is the major structure's displacement

vector,  $\ddot{x}_g(t)$  is the acceleration vector of ground motion, and  $[C_z]$  is the damper's supplemental damping matrix.

In the research, the multi-objective NSGA-II was adopted to optimize the spatial arrangement of dampers in single-span reinforced concrete frame structures for better damping performance<sup>[12]</sup>. The analysis process is illustrated in Fig. 4.

As shown, the NSGA-II-based optimization design for seismic control comprises three major procedures – optimal modeling, structural modeling, and multi-objective genetic searching<sup>[13]</sup>. The optimal modeling determines the design variables and their initial values, optimization objectives, and constraints. Structural modeling involves the building of an analytical model and the simulation of seismic actions. Compared with regular genetic searching, multi-objective genetic searching is characterized by additional population merging and non-dominated sorting and elimination. Also, the latter has a different sequence of steps.

Generally, an optimization model should be established according to the structural characteristics and the seismic control technology applied. Different seismic control technologies are subject to different design variables and their initial values, constraints, and more likely, optimization objectives. As for the optimization of the spatial arrangement of dampers in single-span reinforced concrete frame structures, the primary target is to determine the specific optimal positions of dampers throughout the whole spatial framework so that the given objective function values satisfy the conditions<sup>[14]</sup>. Therefore, two types of optimization can be identified: one defines given objective functions only, without stipulating the number of dampers, and applies the optimizer to locate the positions of dampers that meet the optimization objectives throughout the spatial framework; the other stipulates a given number of dampers and applies the optimizer to generate several arrangement alternatives where the objective function values are as small as possible, and the optimal alternative will be recognized based on overall comparison and consideration in terms of objective functions, economic conditions, and social conditions<sup>[15]</sup>. The latter possesses better feasibility and comparability compared with the former and is chosen for optimization design in this case.

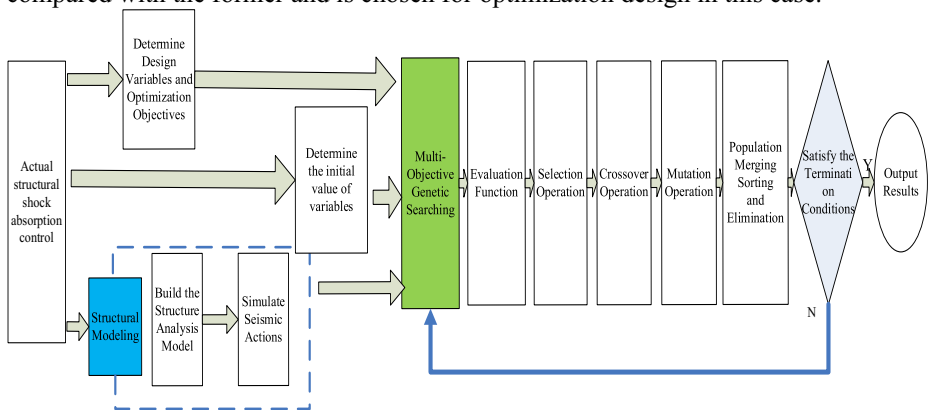


Fig. 4. Optimization of Seismic Control Based on the NSGA-II

## 4 Numerical Calculation

### 4.1 Structural Model

In this section, a single-span reinforced concrete frame structure with 6 storeys (the height of one storey is 3.6 m; the total height is 21.6 m) was used for numerical analysis. The plane layout and the spatial layout are shown in Fig. 5 and Fig. 6, respectively.

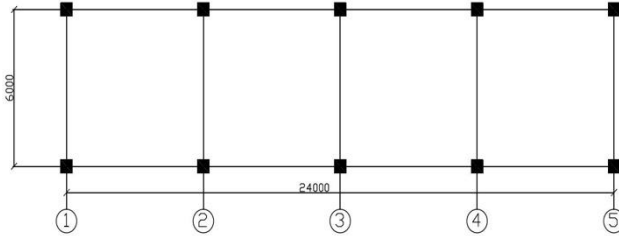


Fig. 5. Plane Diagram of the Structural Model

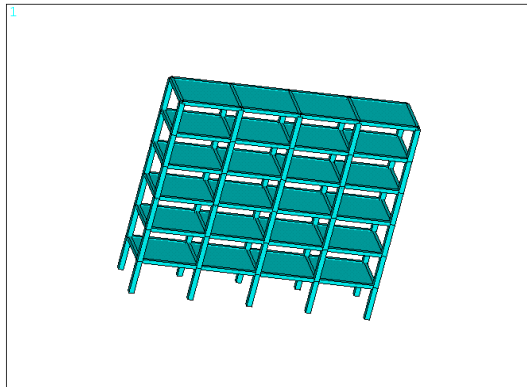


Fig. 6. Space Diagram of the Structural Model

### 4.2 Genetic Coding and Parameters

Parameter determination: Binary is used to encode the chromosome of spatial optimization. A chromosome containing 30 genetic loci is used to represent the arrangement solution requiring optimization<sup>[16]</sup>. A genetic locus bears or does not bear a damper, with {0} indicating negative and {1} indicating positive. The coding is performed from up to down by storey and from left to right by axis. For instance, a gene (10010) can suggest there are 5 potential positions for dampers on the first storey and that two dampers can be deployed in the filler walls on the 1<sup>st</sup> and 4<sup>th</sup> axes, respectively, on the first storey. As for a chromosome containing 30 genetic loci (00010 01010 10010 00010 01010 10000), every 5 genetic loci indicate 5 potential positions for dampers on one storey, and the nine 1s mean that a total number of 9 dampers can be deployed in the filler walls on the 4<sup>th</sup> axis on the 1<sup>st</sup> storey, the 2<sup>nd</sup> and 4<sup>th</sup> axes on the 2<sup>nd</sup> storey, the 1<sup>st</sup>



and 4<sup>th</sup> axes on the 3<sup>rd</sup> storey, the 4<sup>th</sup> axis on the 4<sup>th</sup> storey, 2<sup>nd</sup> and 4<sup>th</sup> axes on the 5<sup>th</sup> storey, and 1<sup>st</sup> axis on the 6<sup>th</sup> storey.

Parameters of the genetic algorithm are  $T=100$ ,  $P_c=0.9$ , and  $P_m=0.1$ , where  $T$  is the number of populations,  $P_c$  is the crossover probability, and  $P_m$  is the mutation probability.

### 4.3 Analysis of the Calculation Results

Two natural waves and one artificial wave were selected for analysis and calculation, and the peak acceleration of ground vibration was adjusted to 70 gal.

Two objective functions aiming at optimizing the spatial arrangement of dampers based on multi-objective optimization include<sup>[17]</sup>:

A. Ratio of the maximum inter-storey drift angle in an energy dissipation structure equipping with dampers to the maximum inter-storey drift angle in a regular structure without dampers under seismic action:

$$f_1(x) = \frac{\theta_{\max}}{\theta_{0,\max}} \tag{3}$$

B. Ratio of the maximum acceleration in an energy dissipation structure equipped with dampers to the maximum acceleration in a regular structure without dampers under seismic action:

$$f_2(x) = \frac{a_{\max}}{a_{0,\max}} \tag{4}$$

where  $\theta_{\max}$  and  $\theta_{0,\max}$  are the maximum inter-storey drift angles with and without dampers, and  $a_{\max}$  and  $a_{0,\max}$  are the maximum accelerations with and without dampers<sup>[18]</sup>.

The viscous dampers with a damping constant of  $C_o = 2.0 \times 10^7 N \cdot s / m$  were adopted<sup>[19]</sup>, and the numbers of dampers were 3, 4, 5, 6, 7, 8, 9, and 10.

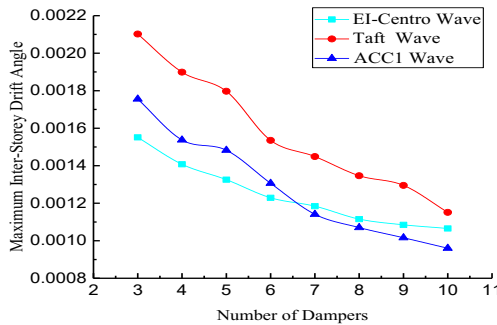
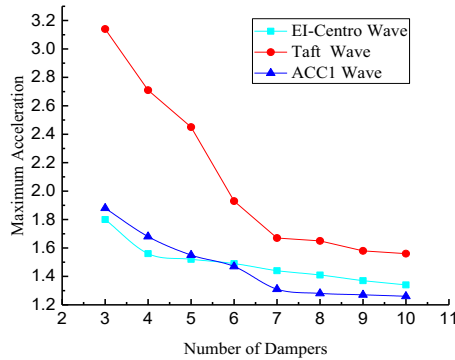


Fig. 7. Correlations of the Maximum Inter-Storey Drift Angles with the Number of Dampers

By virtue of the two objective functions above, the research took into consideration the impacts of both  $f_1(x)$  and  $f_2(x)$  to explore the variation curves of the objective functions with the increasing number of dampers under the EI-Centro wave, the Taft wave, and the artificial wave (Fig. 7 and Fig. 8).



**Fig. 8.** Correlations of the Maximum Accelerations with the Number of Dampers

As evidenced by Fig. 7 and Fig. 8, with the rise in the number of dampers, the structure’s maximum inter-storey drift angles and maximum accelerations decline. When the number of dampers reaches 6 or 7, the downtrends of the maximum inter-storey drift angles and maximum accelerations tend to be moderate. When the number reaches 9 or more, the increment of the damping effect on the two variables is no longer significant.

Determination of final reinforcement schemes: If the number of dampers is stipulated, the statistics of the probabilities of installation position can be drawn up according to the Pareto optimal solutions, and the schemes where the positions are statistically optimal can be regarded as the final reinforcement schemes. Taking the 4-damper reinforcement scheme as an example, the Pareto optimal solutions are shown in Fig. 9 and Table 1.

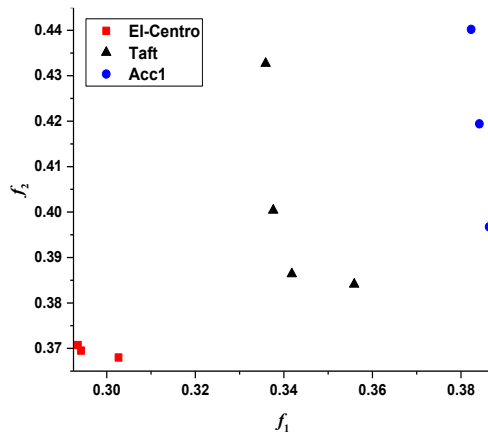


**Fig. 9.** 4-Damper Pareto Optimal Solutions

**Table 1.** Installation Schemes of 4-Damper Pareto Optimal Solutions

Wave Type	Pareto Optimal	Installation Scheme
EI Centro Wave	1	2-3,3-5,4-1,4-5
	2	2-3,2-4,4-2,6-1
	3	2-3,3-4,4-1,4-5
Taft Wave	1	2-3,3-5,4-1,4-5
	2	2-3,2-4,4-4,6-2
	3	1-3,3-5,4-5,5-1
	4	2-4,3-4,4-5,5-2
ACC1 Wave	1	2-3,3-5,4-1,4-5
	2	2-3,2-4,4-4,6-2
	3	1-3,3-5,4-5,5-1

Supposing the structure is reinforced with 4 dampers, the optimizer suggests the same Pareto optimal solution under the three seismic waves. Thus, this specific solution is considered the final reinforcement scheme, which dictates that the 4 dampers are deployed on the 3<sup>rd</sup> axis on the 2<sup>nd</sup> storey, the 5<sup>th</sup> axis on the 3<sup>rd</sup> storey, the 1<sup>st</sup> axis on the 4<sup>th</sup> storey, and the 5<sup>th</sup> axis on the 4<sup>th</sup> storey, respectively. Its damping effects are analyzed based on the two objective functions (Fig. 10-12).

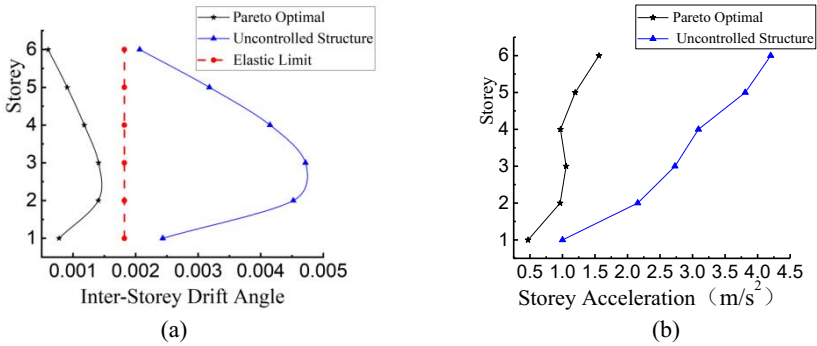


**Fig. 10.** Damping Effect of the 4-Damper Pareto Optimal Solution Under the EI-Centro Wave

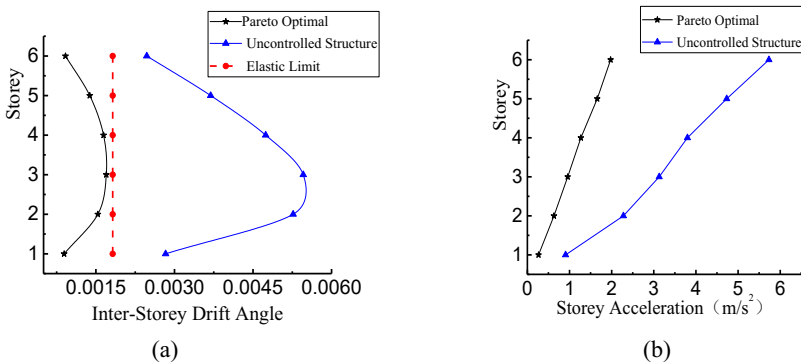


**Fig. 11.** Damping Effect of the 4-Damper Pareto Optimal Solution Under the Taft Wave

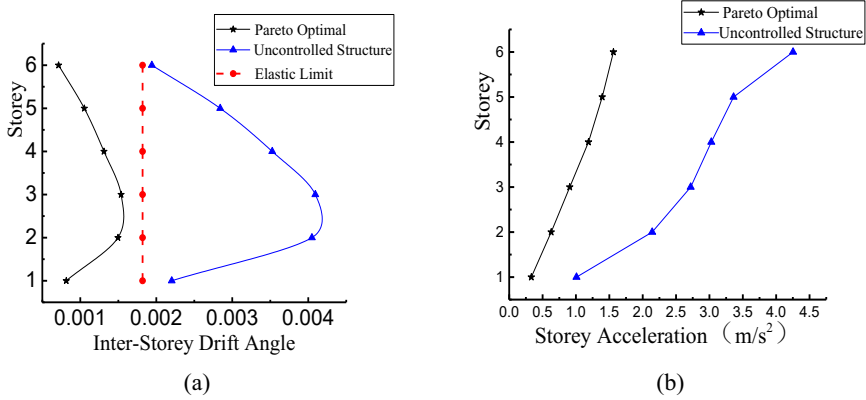


**Fig. 12.** Damping Effect of the 4-Damper Pareto Optimal Solution Under the ACC1 Wave

Supposing the structure is reinforced with 6 dampers, the Pareto optimal solutions suggested by the optimizer under the three seismic waves are summed up in Table 2.

Similarly, the probability statistics are accomplished for all installation schemes in Table 2, and the results are shown in Table 3.

**Table 2.** Installation Schemes of the 6-Damper Pareto Optimal Solutions

Wave Type	Pareto Optimal	Installation Scheme
El Centro Wave	1	1-2,1-4,3-4,4-5,5-1,6-3
	2	1-3,2-5,3-5,4-2,5-2,6-1
	3	2-3,2-4,3-1,4-1,6-2,6-4
	4	1-4,2-3,3-2,4-1,4-2,4-4
Taft Wave	1	1-3,2-3,3-5,4-5,5-1,6-3
	2	1-3,2-4,3-4,3-5,6-1,6-2
ACC1 Wave	1	1-3,2-5,3-5,4-5,5-1,6-2
	2	1-3,2-3,2-1,3-4,4-5,6-1
	3	1-2,1-4,3-5,4-2,6-1,6-2
	4	1-2,2-5,3-3,3-5,6-2,6-4

**Table 3.** Probability Statistics of 6-Damper Pareto Optimal Solutions

Installation Position	Frequency
3-5	6
1-3,6-2	5
2-3,4-5,5-1	4

As for the 6-damper case, the reinforcement scheme suggests that the 6 dampers are deployed on the 3<sup>rd</sup> axis on the 1<sup>st</sup> storey, the 3<sup>rd</sup> axis on the 2<sup>nd</sup> storey, the 5<sup>th</sup> axis on the 3<sup>rd</sup> storey, the 5<sup>th</sup> axis on the 4<sup>th</sup> storey, the 1<sup>st</sup> axis on the 5<sup>th</sup> storey, and the 2<sup>nd</sup> axis

on the 6<sup>th</sup> storey, respectively. The damping effects under the three seismic waves are shown in Fig. 13-15.

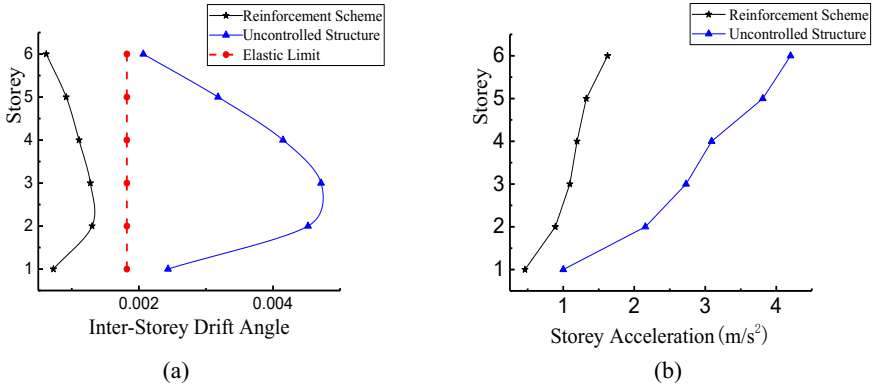


Fig. 13. Damping Effect of the 6-Damper Pareto Optimal Solution Under the EI-Centro Wave

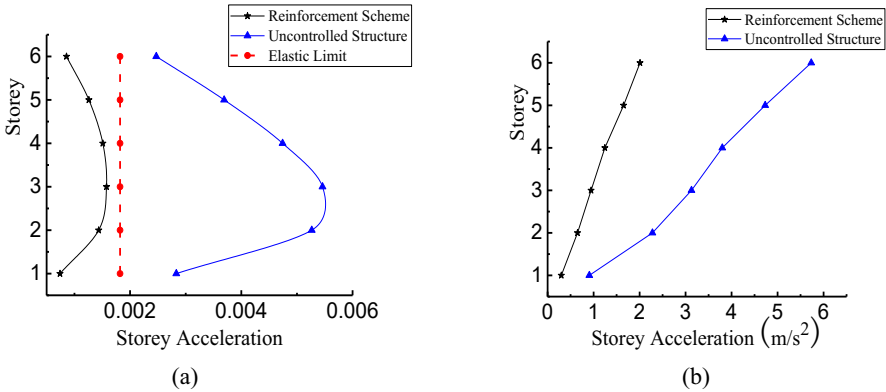


Fig. 14. Damping Effect of the 6-Damper Pareto Optimal Solution Under the Taft Wave

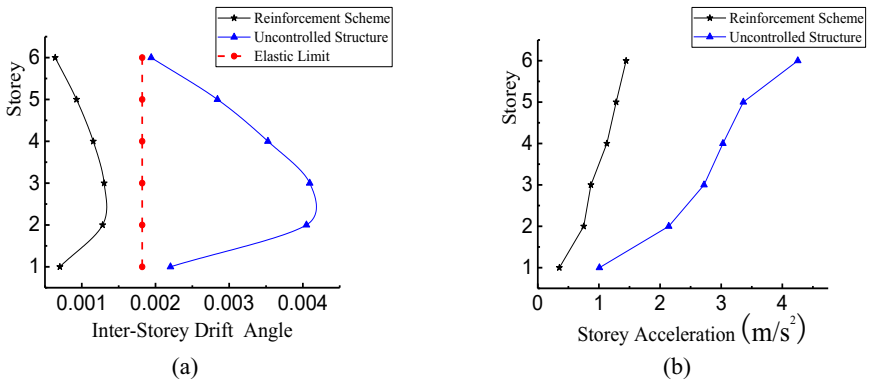


Fig. 15. Damping Effect of the 6-Damper Pareto Optimal Solution Under the ACC1Wave

As shown above, the 6-damper reinforcement scheme determined based on probability statistics has significant damping performance.

## 5 Conclusion

The research prepares an improved multi-objective NSGA-II to optimize the damper-based reinforcement solution for single-span reinforced concrete frame structures required to be reinforced with dampers. Compared with the regular genetic algorithm, the improved multi-objective genetic algorithm can keep the numbers of specific genes in the chromosomes unchanged across generations, which lays the foundation for the subsequent discussion on the correlations of the objective functions with the number of dampers if a damper-based reinforcement scheme is applied. It provides a decision-making basis for more economical reinforcement schemes in practical engineering projects.

In the case of a structure under different seismic waves, when the number of dampers is stipulated, the Pareto optimal solutions proposed by the improved multi-objective NSGA-II can be either the same or different: (1) if the same, the Pareto optimal solution can be reorganized as the final reinforcement scheme; (2) if different, the probability statistics should be applied to identify the most frequent damper positions as the final reinforcement scheme. Nevertheless, according to the objective functions, any reinforcement schemes suggested by the improved multi-objective NSGA-II have significant damping performance.

## Acknowledgment

This research is one of the college-level research programs of Chongqing College of Architecture and Technology in 2023 (2023007).

## References

1. Ou J.P. and Wu B. Analysis and Design of Seismic Retrofit of Beijing Hotel with Energy Dissipators: Time History Method [J]. *Earthquake Engineering and Engineering Vibration*, 2001,21(4):82-87.
2. Chen Z.D., Li A.Q., Zhang Z.Q., et, al. Earthquake-Induced Vibration Control and its Application in Steel Tower on a Reinforced Concrete Tall Building [J]. *Building Science*, 2004, 20(3): 18-23.
3. Zhang Z.Q., Li A.Q., He J.P, et al. The Optimum Parameter Analysis of Mitigating Seismic Vibration of Hefei TV Tower by Applying Viscous Fluid Damper under Earthquake Action [J]. *Earthquake Resistant Engineering*, 2004, (2):39-45.
4. WANG Zilong, REN Wenjie. Research on optimization design for structure with viscous dampers based on genetic algorithm [J]. *World Earthquake Engineering*,2021,37(2):123-131.(in Chinese)

5. CHEN Fengshou, LU Shuhui. Multi-objective optimal arrangement of dampers based on non dominated sorting genetic algorithm-II[J]. *World Earthquake Engineering*, 2023, 39(1):110-117. (in Chinese).
6. Kalyanmoy Deb, Amrit Pratap, Sameer Agarwal, et al. A Fast and Elitist Multi-objective Genetic Algorithm: NSGA-II [J]. *IEEE Transaction Evolutionary Computation*, 2002, 6(2):182-197.
7. ZHOU Yuxian, WANG Shuguang. Research on double-objective synchronous optimization distribution of linear viscous dampers for frame structures [J]. *Journal of Vibration Engineering*, 2023, 36(1):44-51. (in Chinese).
8. QU Ji-ting, YIN Shu-yu, NING Chun-xiao. Optimization of viscous dampers for existing buildings with excessive story drifts[J]. *Earthquake Engineering and Engineering Dynamics*, 2021, 41(1): 92-99.
9. Liu G. Condition Assessment Research to Large-span Bridges Based on Long-term Static Monitoring Data [D]. Chongqing: Chongqing University, 2010.
10. ZHUANG Liang-dong, YANG Yue. The application of genetic algorithm in seismic performance optimization of Y-shape eccentrically braced composite frame [J]. *Engineering Mechanics*, 2023, 40(7): 185 – 195. (in Chinese)
11. MA Hongwei, WANG Junjie, WEI Zengting. Design method of energy dissipation system with viscous damper based on coarse-grained-master-slave parallel genetic algorithm [J]. *Building Structure*, 2023, 51(s1):924-930. (in Chinese)
12. Oreski S, Oreski D, and Oreski G. Hybrid System with Genetic Algorithm and Artificial Neural Networks and Its Application to Retail Credit Risk Assessment. *Expert Systems with Applications*, 2012, 39(16):12605-12617.
13. Xu Q.Y., Li A.Q., Ding Y.L., et al. Research on Location Optimization of Energy Dissipation Braces Between Columns of Long-Span Hangar Based on Improved Genetic Algorithm [J]. *China Civil Engineering Journal*, 2013, 46 (6):35-43.
14. GAO Feifan. Research on optimization of mixed arrangement for different damper energy dissipation systems based on genetic algorithm [D]. Xi'an: Xi'an University of Architecture and Technology, 2018. (in Chinese)
15. ZHAO J, LI K, ZHANG X C, et al. Multidimensional vibration reduction control of the frame structure with magnetorheological damper[J]. *Structural Control and Health Monitoring*, 2020, 27 (8): e2572.
16. Tabar S F, Ashtari P. Simultaneous size and topology optimization of 3D outrigger-braced tall buildings with inclined belt truss using genetic algorithm [J]. *Department of Civil Engineering, University of Zanjan, Zanjan, Iran*, 2020(29): 38-40. e1776-1791.
17. Wang L L, Zhao X et. A practical fractional numerical optimization method for designing economically and environmentally friendly super-tall buildings [J]. *Applied Mathematical Modelling*, 79(2020), 934-953.
18. S. Prakash, R. S. Jangid. Optimum parameters of tuned mass damper-inerter for damped structure under seismic excitation. *International Journal of Dynamics and Control*, 2022, 23(12):193-198.
19. Y. S. Erdogan, M. Ada. A Computationally Efficient Method for Optimum Tuning of Single-Sided Pounding Tuned Mass Dampers for Structural Vibration Control. *International Journal of Structural Stability and Dynamics*, 2021, 21(5):1-16.

**Open Access** This chapter is licensed under the terms of the Creative Commons Attribution-NonCommercial 4.0 International License (<http://creativecommons.org/licenses/by-nc/4.0/>), which permits any noncommercial use, sharing, adaptation, distribution and reproduction in any medium or format, as long as you give appropriate credit to the original author(s) and the source, provide a link to the Creative Commons license and indicate if changes were made.

The images or other third party material in this chapter are included in the chapter's Creative Commons license, unless indicated otherwise in a credit line to the material. If material is not included in the chapter's Creative Commons license and your intended use is not permitted by statutory regulation or exceeds the permitted use, you will need to obtain permission directly from the copyright holder.

